Polymer Journal (2019) 51:199–209
https://doi.org/10.1038/s41428-018-0141-8

ORIGINAL ARTICLE

# Elongation induced β- to α-crystalline transformation and microvoid formation in isotactic polypropylene as revealed by time-resolved WAXS/SAXS

Hideo Kurihara[1] · Shinichi Kitade[1] · Kazuyuki Ichino[2] · Isamu Akiba[3] · Kazuo Sakurai[3]

Received: 17 August 2018 / Revised: 18 September 2018 / Accepted: 19 September 2018 / Published online: 29 October 2018


## Abstract

Time-resolved synchrotron small- and wide-angle X-ray scattering (SAXS) and (WAXS) was carried out during the high-speed elongation of unoriented exclusively β-crystal-containing isotactic polypropylene, and the results were compared with those for α-crystal polypropylene. SAXS and WAXS indicated that there were three different stages in the deformation. In the first stage, microvoid formation started at the upper yield point, which is associated with lamellae perpendicular to the elongation. In the second stage, the meridional β-lamellar SAXS disappeared; the second stage results in a β–α polymorphous transformation that produces a highly oriented α-crystal parallel to the elongation direction. In this stage, equatorial SAXS remained intact mainly because of microvoid formation. In the third stage, we observed decreasing equatorial SAXS and re-emerged meridional SAXS. After the disappearance of the parallel lamellae, which indicates the depletion of the source for the β–α transformation, the remaining perpendicular lamellae became the transformation source. The perpendicular lamellae underwent inter- and intralamellar slipping and fragmentation and then unfolded to produce the oriented α-crystal. The β-crystal film contained many microvoids, which absorbed the stress. This means that the β- and α-crystals may not have been fully subjected to the applied stress, causing lower orientations for the α-crystals and the remaining β-crystals.

## Introduction

Polypropylene (PP) is a crystalline thermoplastic polymer that is widely used in various molding processes because of its excellent mechanical properties and chemical resistance. Generally, commercially available PPs contain >98% isotactic polypropylene (iPP), which means the iPP portion determines the overall properties. [1] One of the characteristic properties of iPP is rather high polymorphism; specifically, there are three crystal structures: stable α- (monoclinic), metastable β- (hexagonal), and γ-crystals (orthorhombic). [2] Furthermore, iPP adopts a stable mesomorphic phase, [3] of which the most commonly observed is α-crystal [2]. β-crystal is formed by adding a specific nucleating agent [4, 5] or applying high shear during injection molding. [6] β-crystal is transformed into α-crystal by annealing at high temperatures (generally above 140 °C) or by mechanical deformation such as elongation. [7, 8] This β–α polymorphous transformation is well studied [9, 10] because of its practical importance and fundamental interest. When commercial PP is used in injection molding, some portion of the finished product contains β-crystal, normally at locations where relatively high shearing was applied during the molding. β-crystal is less rigid than α-crystal, and thus, the β-crystal portion may cause a lack of mechanical uniformity in the finished product. Despite its lower rigidity, β-crystal-containing iPPs (β-iPPs) have several advantages, such as high impact strength, toughness, and ductility; in additionally, they easily form microvoids. These advantages have been exploited for several purposes, including for separator films in batteries [11, 12].

In other words, intrinsically loose β-crystal lamellae exhibit weak resistance to externally applied stress, causing

✉ Hideo Kurihara
Kurihara.Hideo@md.pochem.co.jp

[1] Research and Development Division, Japan Polychem Corporation, 1 Toho-cho, Yokkaichi, Mie 510-0848, Japan

[2] Research and Development Division, Japan Polypropylene Corporation, 1 Toho-cho, Yokkaichi, Mie 510-0848, Japan

[3] Faculty of Environmental Engineering, The University of Kitakyushu, 1-1 Hibikino, Wakamatsu, Kitakyushu, Fukuoka 808-0135, Japan

the simultaneous occurrence of microvoid formation and β–α polymorphous transformation. [10] The final morphology of β-iPPs strongly depend on the deformation speed, annealing conditions, and temperature. For example, in the battery separator example, the ideal pore size to allow ions to flow through while preventing the passage of other components can be achieved by optimizing the above variables. Therefore, the β–α transformation that occurs under deformation (such as elongation) is an important issue, especially under the conditions used in production plants. However, it has not yet been clarified how this transition occurs and which conditions are essential for it. In the work reported here, we studied the β–α transformation at a relatively high elongation speed (ca. 10 mm/min) using synchrotron time-resolved wide-angle X-ray scattering (TR-WAXS) and small-angle X-ray scattering (TR-SAXS). To the best of our knowledge, no TR-SAXS/WAXS studies have previously been performed at such a high elongation rate.

Opto-rheometry, transmission electron microscopy (TEM), and scattering have been applied to observe the deformation of β-iPPs [13, 14]. It has normally been observed that both interlamellar slipping, which is caused by deformation of the amorphous domain in the crystalline domain, and lamellar twisting occur during the deformation of β-iPPs, although intralamellar slipping (separation or fragmentation of the crystalline domain) dominates in α-iPPs [8, 12]. For the β–α transformation, two mechanisms have been proposed: one involves stress-induced melting in the neck region followed by recrystallization to α-crystal (melting/recrystallization process), whereas the other involves the unfolding of β-lamellae (i.e., chain withdrawal from the lamellae) leading to chain alignment owing to the shear and α-crystal formation (solid-to-solid martensitic phase transformation). [14, 15] Although there have been many studies, the molecular mechanism of the β–α transformation is still under debate. According to a recent review, [16] the most general and important micromechanical model of plastic deformation is a crystallographic model based on thermal activation of screw dislocations with the Burgers vector parallel to the chain axis. This screw dislocation model clearly explains the decrease in stress after the high yield point. On the other hand, the stress-induced melting and recrystallization fit to the constant-stress region (i.e., drawing) because there is no energy dissipation in this model. This screw dislocation model may be help in understanding the β–α transformation. Furthermore, the lamellar clustering process [17] proposed by Nitta and Takayanagi is considered essential in the yielding process of β-iPPs, where the β–α transformation occurs. Here, the lamellar clustering process involves the formation of small-lamella crystal units (which result from intralamellar slipping) and tie molecules connecting the crystal units around the upper yield point, irreversible dislocation of the crystal units, and rearrangement in the direction of drawing during the drawing process. The mechanism of the β–α transformation may be reconsidered with the incorporation of the lamellar clustering process.

Phulkerd et al. [18] carried out TEM and WAXS for a one-directionally stretched PP sheet that had previously been mixed with *N,N′*-dicyclohexyl-2,6-naphthalenedicarboxamide as a β-crystal nucleating agent and extruded from a T-die. They found that the c-axis of the β-crystals oriented perpendicularly to the direction of flow. This is because the rod-like nucleating agents were aligned parallel to the direction of flow, and the β-form crystallized epitaxially from the surface of the agent. When they elongated the sheet perpendicular to the flow, the β-crystals oriented in the direction of elongation, and β–α transformation occurred without void formation. Although this is an interesting result, the stretching speed used was not as fast as that in practical processing. More recently, Chen et al. [19] studied the influence of oriented β-crystals on deformation behavior by using TR-SAXS/WAXS. They found that the oriented β-crystals promoted the earlier occurrence and delayed enlargement of microvoids and that microvoid formation may be induced by the separation or slipping of oriented β-crystals, which occurs earlier than β–α transformation.

## Experimental

### Materials and sample film preparation

Homo PP polymerized with Zieglar-Natta catalyst (grade FY4H; Japan Polypropylene Corporation) was used in this study. Its melt flow index was 5 g/min (at 230 °C and 2.16 kgf), and its molecular weight was $\sim 2.8 \times 10^5$. As a β-nucleating agent, we used NJSTAR NU-100 (New Japan Chemicals Co., Ltd.), which is *N,N′*-dicyclohexylnaphthalene-2,6-dicarboxamide. The β-nucleating agent (0.1 wt%) was melt-blended with the PP sample using a twin-screw extruder at 230 °C.

The PP pellets were heated to 210 °C, compressed to 0.2 mm, and kept under these conditions for 3 min, followed by cooling to room temperature. This process caused the formation of an α-crystal with crystallinity of ~ 52%, as determined by WAXS. Hereafter, we refer to this film as α-film. When β-nucleating agent-containing PP pellets were treated in the same manner, a film with 58% crystallinity was obtained, and the β-crystal/α-crystal ratio was determined to be approximately 90/10 by the Turner-Jones method [7]. This film is termed β-film. Each film was cut into strips of 10 mm in width for in situ time-resolved SAXS/WAXS, where SAXS refers to small-angle X-ray scattering, or cut into a dumbbell shape (JIS K7162-5A).

The dumbbell-shaped films were elongated by a microtensile testing machine with a thermocontrolled air atmosphere bath (IMC-18E0; Imoto Machinery Co. Ltd., Japan) to 150% (with an initial cross-head distance of 40 mm and cross-head speed of 10 mm/min) at 115 °C. These samples were used for position scan measurement.

### In situ time-resolved SAXS/WAXS measurements under elongation

During the elongation in the temperature range of 115–145 °C, in situ time-resolved SAXS and WAXS measurements were carried out using a microtensile testing machine (IMC-18E0) at the BL03XU beamline [20, 21] in the synchrotron radiation facility at SPring-8, Hyogo, Japan (proposal Nos. 2015A7218, 2015B7269, 2016A7218, 2016B7268). This machine has two movable sample clamps, and the X-ray beam position was set as the middle position between two clamps, i.e., the center position of the sample. The sample was elongated in the opposite direction at the same speed, and thus, the X-ray beam always hit the sample in the same position. The elongation speed was 10 mm/min, and the maximum elongation was 200%. The X-ray beam was ~ 200 × 200 μm in size, and a flat panel detector and an image intensifier + charge-coupled device camera were used to acquire WAXS and SAXS patterns. [20] The time interval was 1.0 s, and the exposure time was 0.5 s, meaning that the data were obtained at strain intervals of 1.67%. Although this was the shortest interval that could be determined by the detector, this resolution may not be sufficient to trace the crystallization of iPP because most changes appear within the strain range of a few percent around the yield point.

### Ex situ SAXS/WAXS and TEM measurements

We carried out position scan measurement by using an X-ray beam 30 × 30 μm in size for the elongation of the dumbbell-shaped films at the same beamline. TEM was carried out with a JEM-2100F (JEOL Ltd., Japan). The sample was stained with $RuO_4$ to enhance the image contrast and cut to a thickness of ~ 100 nm using a microtome.

## Results and discussion

### In situ SAXS/WAX time-resolved measurements

#### α-Crystal deformation

The upper panel of Fig. 1 shows the stress–strain curve when the α-film was elongated at 10 mm/min and 115 °C and indicates how the 2D WAXS and SAXS images changed at the indicated strain points (a0, 0%: before elongation, a1, 16.7%: upper yield point, a2, 40%: lower yield point, a3, 100%: during yield plateau). Notice that necking passed the X-ray-irradiation point between a2 and a3 and that the SAXS/WAXS images after necking were contrast-enhanced almost 1.5-fold. At a0, five major diffraction circles were observed; they were $(110)_\alpha$, $(040)_\alpha$, $(130)_\alpha$, $(111)_\alpha$, and $(-131)_\alpha + (041)_\alpha$ from the α-form monoclinic iPP crystal, where the subscript alpha indicates the lattice indices for the α-crystal. At a1, there appeared to be no appreciable changes in either WAXS or SAXS, but as shown later, the long period of the meridional direction increased while that of the equatorial direction remained constant (see Fig. 3). This is consistent with previously reported results [22]. These findings can be explained by the applied stress elastically elongating the interlamellar tie chains parallel to the direction of elongation. At a2 (40%, plastic region, after necking, contrast-enhanced), there was no change in the WAXS pattern, but SAXS showed that the circular halo had become ellipsoidal in shape; the meridional scattering shifted to a lower $q$, and four relatively strong scattering patterns (clover pattern) appeared at an angle of ~ 30° off the equatorial direction. This indicates the orientation of the lamellae. At a3, WAXS showed that four arc-like diffractions from $(110)_\alpha$, $(040)_\alpha$, and $(130)_\alpha$ were allied in the equatorial direction, as well as at higher angles, and the $(111)_\alpha$ and $(-131)_\alpha + (041)_\alpha$ diffractions converged to the arc-like ones at an angle of 45° off the equatorial direction. Accompanying these WAXS changes, SAXS showed two scattering points in the meridional direction as well as the shifting of the peak position to a lower $q$. These results are typical patterns for c-axis orientation in the direction of elongation owing to the formation of a fibrillar-like crystal [17].

Here, we will explain why the contrast of the SAXS image was enhanced. At a0, the degree of crystallinity was ~ 50%. In the case of the ideal two-phase model, which is a good approximation for partially crystalline polymers, the sum of the scattering intensities: invariant is proportional to $V\Delta\eta^2\phi_a\phi_c$, where $V$ is the scattering volume; $\Delta\eta$ is the contrast, which in our case is proportional to the difference in density between the amorphous and α-crystal; $\phi_a$ and $\phi_c$ are the volume fractions of the amorphous and α-crystal phases, respectively; and $\phi_a$=1-$\phi_c$. By comparing a0 and a4, we can see that $V$ decreased by ~ 50%, whereas $\phi_c$ and $\phi_a$ are almost the same (not shown). These changes may result in a 50% reduction in the invariant.

For α-film, major changes in both SAXS and WAXS occurred between the upper yield point and 50% strain. Further SAXS and WAXS images in this range (by 5%) are compared in Fig. 2a, b, respectively. At 20% strain, SAXS showed a clover pattern that was retained until 40%. This clover pattern then changed to meridional scattering at 45%; only meridional scattering remained at 50%. During the

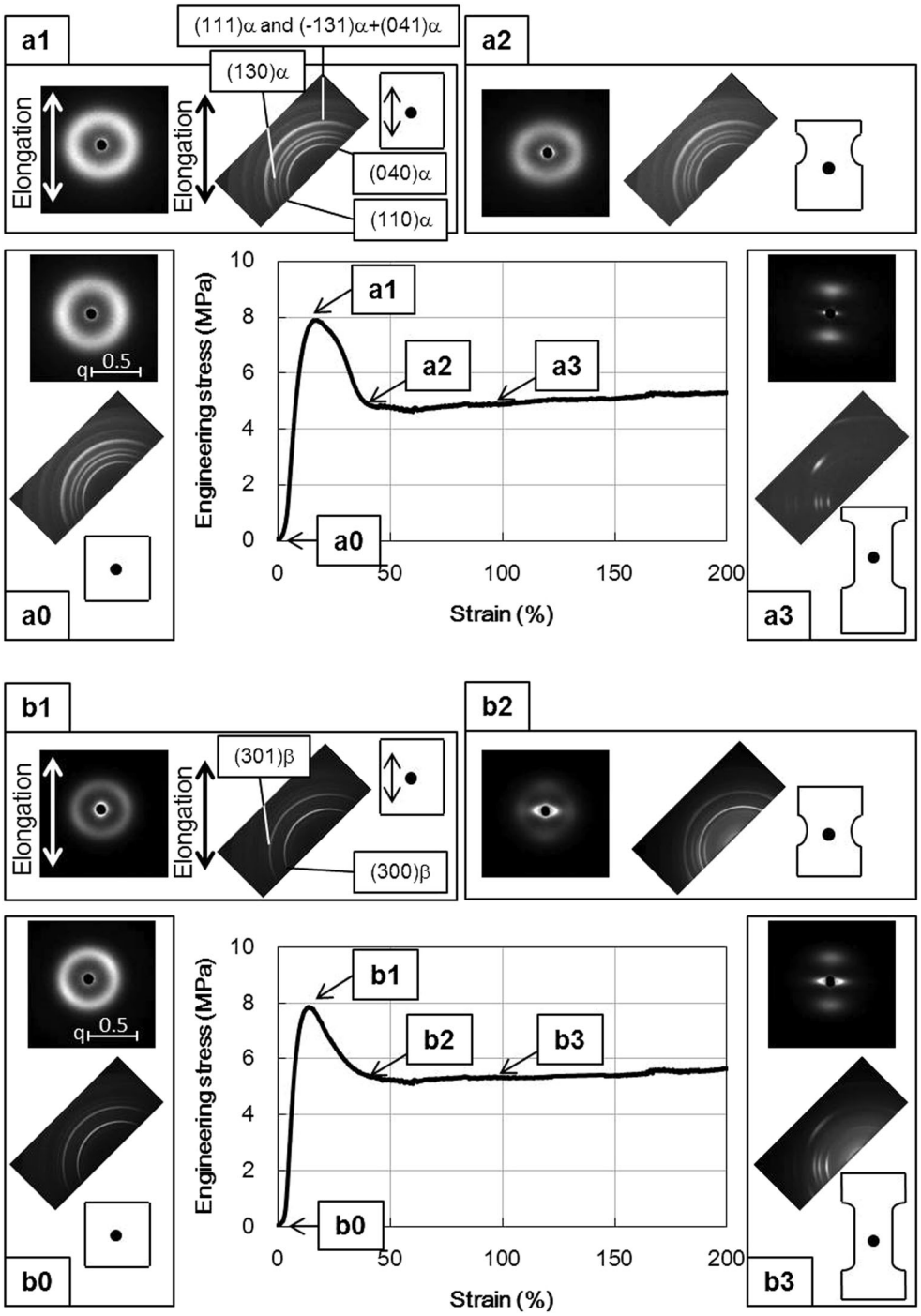


**Fig. 1** Stress–strain curves for the α- (upper) and β-films (lower) and the SAXS and WAXS patterns for the selected strain points as well as a schematic of the sample shape and the point of X-ray irradiation

necking, WAXS did not change markedly until the strain reached 45%. At 45%, the c-axis orientation started to develop because the $(111)_\alpha$ and $(-131)_\alpha + (041)_\alpha$ diffraction became more intense at an angle of ~45° off the equatorial direction. The c-axis orientation occurred between 45 and 50%; clearly, the crystal orientation was delayed compared with the long period orientation. The long periods calculated from the SAXS are plotted against the strain in Fig. 3a, b. The average distances between the lamellae in the equatorial direction did not change at all, but those in the direction of elongation increased with an increase in strain. It is interesting that such an increase was

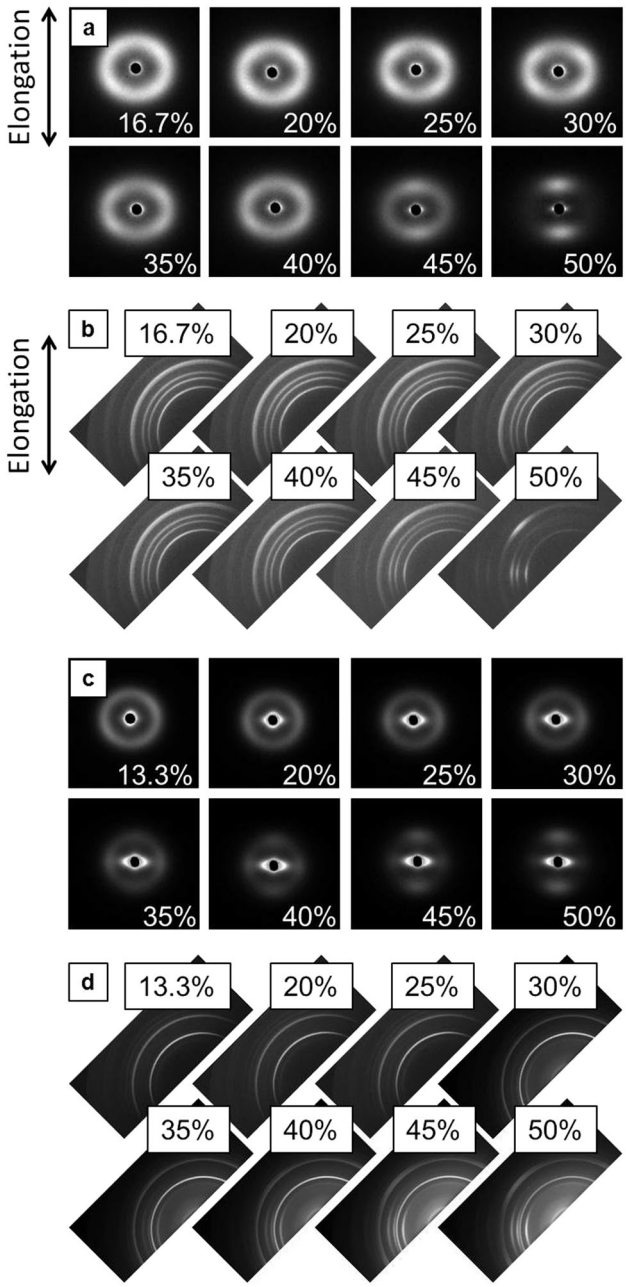


**Fig. 2** Comparison of the SAXS and WAXS patterns for the selected strain points of the α- and β-films

observed even before the upper yield point; this can be ascribed to elongation of the amorphous tie chains between the lamellae. Fig. 3c, d plot the relative SAXS intensities determined by $(I_{\pm 10}/I_{\pm 360})$, where $I_{\pm 10}$ and $I_{\pm 360}$ are the normalized SAXS intensities in the range of ±10° off the meridional or equatorial direction and the circular averaged intensity, respectively. The intensity was also averaged in the range of $0.17\,\mathrm{nm}^{-1} < q < 0.80\,\mathrm{nm}^{-1}$. At strain 0%, the intensities of the α-and β-film are different. It is believed that a low degree of orientation remained at the time of the sample preparation. The meridional and equatorial SAXS intensities remained almost constant up to 40% strain, whereas the former increased and the latter decreased between 40 and 50% strain; this is consistent with the orientation of the fibril–lamellae.

Although we did not perform direct observations, we can reasonably assume that there were well-grown α-crystal spherulites at a0, with stacked lamellae accompanying the daughter lamellae. When stress is applied, the tie chains between the lamellae are elastically elongated until the upper yield point. As shown in Fig. 3a, the increasingly long spacing in the meridional direction is related to this elastic tie-chain elongation. After the yield point, the clover pattern appears, indicating that intralamellar slipping causes tilting of the lamellar chains and rotation of the lamellae themselves. In the necking region, shear banding occurs, and the band direction is ~45° off the direction of elongation. This band causes the lamellar orientation that leads to the clover pattern. This may explain why SAXS started to change earlier than WAXS. Furthermore, during the shear band formation, the lamellae may be fragmented into lamellar clusters and slip with each other. The clover pattern may reflect the special arrangement among these lamellar clusters. These changes are irreversible catastrophic events. The tie chains have already been stretched after necking, and the applied stress causes an orientation of the lamellar clusters or fragmented crystalline in which the c-axis becomes parallel to the direction of elongation. At 50% strain, the lamellae are also stacked in the direction of elongation. Therefore, we conclude that all of the changes in TR-WAXS/SAXS are consistent with the typical tensile plastic deformation of semicrystalline polymers.

## β-Crystal deformation

The lower panel of Fig. 1 shows the stress–strain curve and TR-WAXS/SAXS 2D images of the β-film under the same conditions along with the same four strain points as for the α-film; here, there was no contrast enhancement and the necking passed between b1 and b2. At b0, strong isotropic $(300)_\beta$ and $(301)_\beta$ diffraction from the β-crystal was observed, confirming that the addition of NJSTAR NU-100 caused the complete suppression of α-crystal crystallization. The β-film stress–strain curve is slightly different from that of the α-film; specifically, the upper yield profile is narrower than that of the α-film, and the lower yielding point seems to appear earlier than for the α-film. These features are related to the loose β-crystal; namely, in the β-crystal, chain withdrawal and chain slipping easily occur. At b2, dramatic changes were observed in both SAXS and WAXS. SAXS showed rather intense central scattering in the direction perpendicular to elongation, indicating that the elongation created voids in the film. [19] Furthermore,

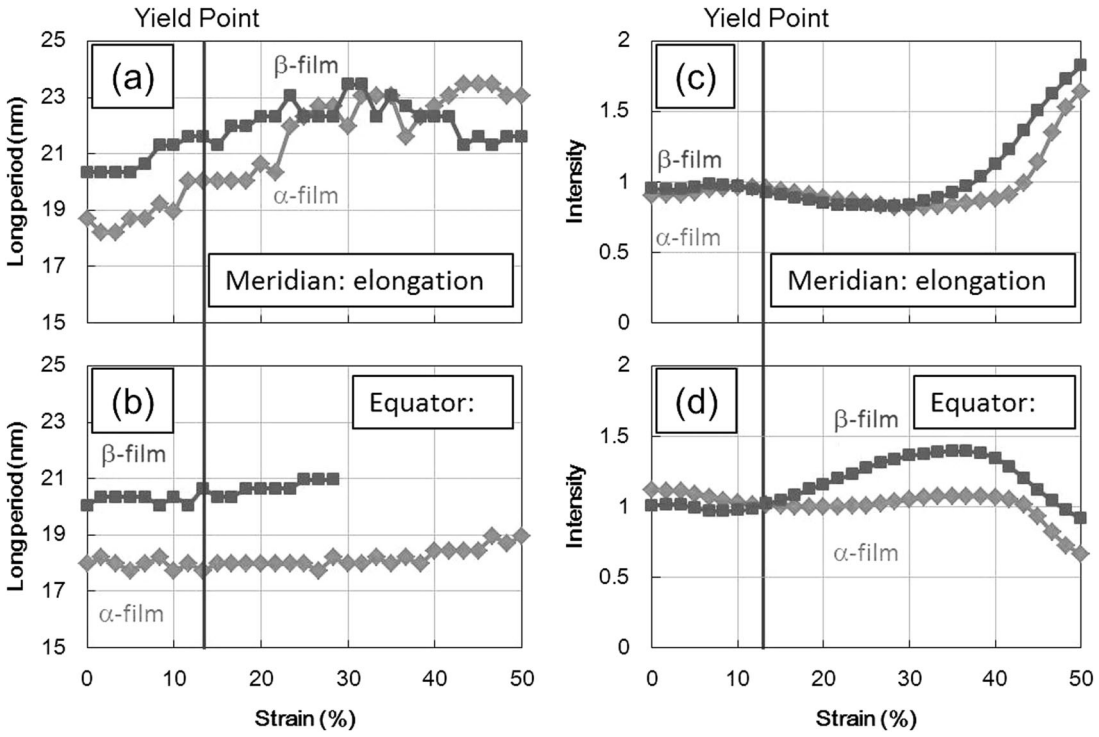


**Fig. 3** Long period distance change in the equatorial **a** and meridional **b** directions. The normalized SAXS intensity changes in the equatorial **c** and meridional **d** directions. The red lines indicate the upper yield point

broad and weak arc-like scattering appeared in both the meridional and equatorial directions. WAXS consisted of a mixture of α- and β-crystals: anisotropic $(110)_\alpha$, $(040)_\alpha$, and $(130)_\alpha$ appeared while $(300)_\beta$ remained, but no orientation of the β-crystal was observed. (The diffractions $(111)_\alpha$, $(-131)_\alpha + (041)_\alpha$ for α-crystal and $(301)_\beta$ for β-crystal are overlapped, so it is hard to distinguish between them.) When we carefully examined the WAXS images, it was clear that the principal diffraction of α-crystal was oriented perpendicular to the elongation. This suggests that, once the β-crystal was subjected to stress due to elongation, it immediately changed to α-crystal, which showed the c-axis orientation in the direction of elongation. At b3, WAXS showed that β-crystal diffraction almost disappeared; we observed a crystalline-lamella orientation similar to that of the α-film. SAXS showed that the voids remained, but their more intense, streak-like shape indicates that they were probably enlarged in the direction of elongation.

### The initial stage of β-crystal deformation: microvoid formation

Again, the major changes in both SAXS and WAXS in the β-film occurred between the upper yield point and 50% strain. SAXS and WAXS images in this range are shown for comparison in Fig. 2c, d, and the long periods and their intensities are plotted against the strain in Fig. 3. The meridian long period started to increase before the yield point and reached a maximum at 30%. The microvoid peaks emerged at 20% strain, earlier than the long spacing and much earlier than the formation of oriented α-crystal owing to β–α transformation. This microvoid SAXS became more intense with increasing strain, which is consistent with the findings of Chen et al. [20] They explained that microvoid formation occurs earlier than lamellar orientation owing to β-lamellar slipping followed by lamellar dislocation, which provides an opportunity for the formation of microvoids in the direction of elongation. They identified an interesting phenomenon: when the c-axis of the β-crystal was oriented perpendicular to the direction of elongation (the lamellar stacking was also perpendicular to the elongation, giving equatorial scattering), the occurrence of microvoid formation was promoted. This suggests two important points: first, microvoids are formed in amorphous domains between or near these perpendicular lamellae. Second, the lamellar stacking parallel to the elongation (i.e., when the β-crystal c-axis is parallel to the elongation as shown by meridional SAXS) may lead to the dissipation of the strain energy without microvoid formation. This energy dissipation is probably related to chain unfolding or chain withdrawal from the crystal or chain slipping in the crystal because of the looseness of the β-crystal. This is because the stress

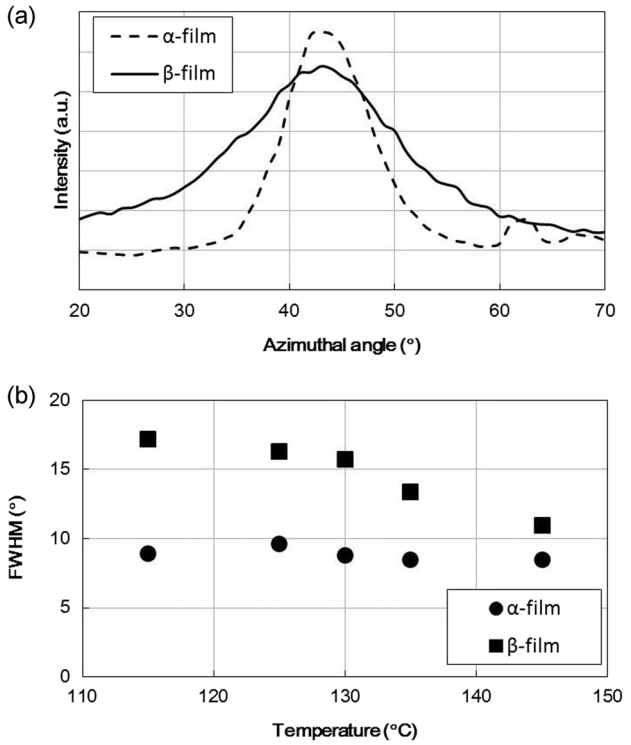


**Fig. 4** Comparison of the α-crystal orientation. **a** The dependence on the azimuthal angle of the diffraction intensity of $(110)_\alpha$ at 115 °C. **b** The dependence on the elongation temperature of the full width at half maximum (FWHM) for azimuthal profiles of $(110)_\alpha$ at 200% strain

direction is parallel to the c-axis, which means that chain unfolding and withdrawal occur more easily than with the perpendicular alignment.

### The second stage of β-crystal deformation: remaining equatorial SAXS

At 25% strain, there was a clear overlap of equatorial scattering with weak circular scattering in SAXS. In WAXs, there was diffraction from the transformed oriented α-crystal as well as the unoriented β-crystal. At 35% strain, the SAXS meridional scattering became slightly weaker, but the equatorial scattering became more intense, as shown in Fig. 3c, d. Comparing the 25%, 30%, 35%, and 40% strains, there was more clearly oriented α-diffraction at higher strain levels. The equatorial SAXS appeared to peak at ~35% strain, as shown in Fig. 3d. We can assume that the cause of the equatorial SAXS from 20 to 40% is lamellar stacking perpendicular to the elongation, which is associated with microvoid formation. The microvoids are formed near the perpendicular β-lamellae, most likely the amorphous domain β-intralamellae. The microvoids may not destroy the β-lamellae. The surviving perpendicular β-lamellae can provide the equatorial SAXS scattering. These β-lamellae remain almost intact at strains up to 40%. In contrast to the equatorial SAXS, the meridional SAXS decreased with a change in strain from 20 to 30% and then increased at 35% (as in Fig. 3c). The cause of this decrease in meridional SAXS is that the β-lamellae stacked parallel to the direction of elongation. They are expected to easily undergo chain unfolding from the crystal and lamellar slipping, so separation and fragmentation of the lamellae may occur. We can assume that once the chains have withdrawn from the crystal, they are transformed into α-crystal immediately. From the present data, we cannot determine whether this occurs through melt-crystallization or solid-to-solid transformation. β–α transformation is the reason for the decreasing intensity of the meridional SAXS. The reincreasing intensity of meridional SAXS at 35–40% strain may be owing to the newly formed α-lamellae parallel to the direction of elongation. The changes in SAXS from 25 to 40% strain, namely, decreasing meridional and maintained equatorial scattering, indicate that the perpendicular β-lamellae were associated with microvoid formation and remained intact, whereas the parallel β-lamellae were the source of the β–α transformation. In Fig. 3a, the long period decreases starting at ~40% elongation. This is consistent with the point where the transition from β-crystal to α-crystal takes place. In other words, it seems that the melting recrystallization of β-crystal occurred at this point. Therefore, it is thought that the force applied to the β-crystal by elongation is relaxed and the long period decreased.

### The third stage of β-crystal deformation: formation of fibril-like α-lamellae

At 50% strain, the equatorial SAXS almost disappeared and the meridional SAXS returned, but its position shifted to the low-$q$ region. WAXS clearly showed that the oriented α-crystal and re-emerged meridional SAXS scattering could be assigned to the long spacing of the newly formed α-crystal lamellae that were oriented parallel to the direction of elongation. The changes above 50% strain contrasted with those below it. Specifically, the disappearance of meridional scattering represents the depletion of the source of the β–α transformation and a lack of a route for strain energy dissipation. At this stage, the perpendicular β-lamellae have to deform. The inter- or intralamellar slipping or lamellar rotation prompts the rearrangement and deformation of the perpendicular β-lamellae. These deformed lamellae become the new source of β–α transformation.

In the WAXS results at 50% strain (Fig. 2), the α-crystal orientation was much higher in the α-film than in the β-film, which is confirmed in Fig. 4. Here, the dependence of the diffraction intensity of $(110)_\alpha$ on the azimuthal angle is compared between the α- and β-films at a strain of 200% and temperature of 115 °C in the upper panel and the full width at half maximum of $(110)_\alpha$ is plotted against

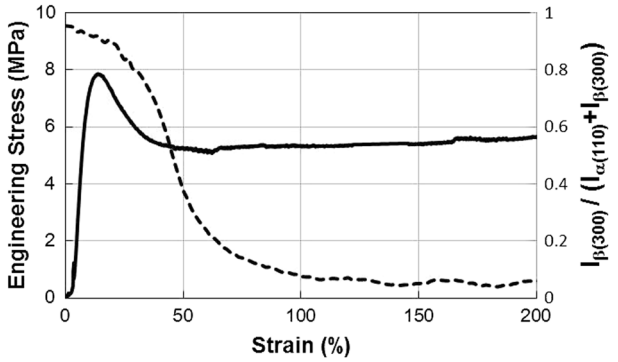


**Fig. 5** Time course of the α/β crystal ratio in the β-film elongated at 115 °C determined by the WAXS intensity ratio $I_{(300)_\beta} / \left[I_{(110)_\alpha} + I_{(300)_\beta}\right]$, compared with the stress–strain curve

elongation temperature in the lower panel. The upper panel confirms the higher orientation of the α-crystal in the α-film than in the β-film. The lower panel indicates that the orientation of the β-film increased with increasing temperature and appeared to reach the same level as that of the α-film at 145 °C, whereas that of the α-film remained almost constant. The β–α transformation occurred at a higher temperature. When there was no stress, the transformation occurred above 140 °C, but this temperature may decrease under stress. Therefore, increasing orientation with increased temperature is owing to the increased and enhanced formation of the α-crystal at higher temperatures. Once the α-crystals form, they should behave in the same manner as in the α-film and not form microvoids, regardless of stress.

### Slow process of β–α transformation

As shown above, the α-crystal orientation is lower in the β-film than in the α-film when they are elongated under the same conditions. At 50% strain, there were a large number of β-crystals remaining in the film. This indicates that a certain portion of the β-film was not fully subjected to the stress applied by elongation. We assume that a large amount of the applied stress goes to the microvoids and the deformation of the microvoids causes dissipation of the energy. In fact, the microvoid scattering at the center became more intense with increasing strain. We determined the α/β ratio from the averaged intensities by using the relation $I_{(300)_\beta} / \left[I_{(110)_\alpha} + I_{(300)_\beta}\right]$ and plotted it (Fig. 5) to compare it with the stress–strain curve of the β-film. The findings showed that β–α transformation gradually proceeded from the highest yield and continued to occur under the drawing process until the strain reached 150%. This slow process may be related to the microvoids formed upon necking. The formation of voids leads to dissipation of the strain energy at necking, and the deformation of voids leads to the dissipation of the strain energy at drawing. The β-crystal is transformed to α-crystal during the drawing, but the α-crystallite in the β-film is under different stress conditions than the α-crystallite in the α-film. Because of the presence of microvoids, the stress applied to the α-crystallite in the β-film is less than that of the α-crystallite in the α-film; this lower stress may not induce intralamellar slipping. The crystallinity remained rather high during the whole process, and the formation of the α-crystallite occurred quite rapidly. This transformation started at the yielding point and continued during drawing because the net stress applied to the crystallites was presumably small owing to the voids, which caused a slow recrystallization process without leading to fragmentation of the crystals. [23]

## Ex situ SAXS measurements

The above-mentioned time-resolved measurements may lack the resolution needed to provide detailed information. Specifically, the data obtained at strain intervals of 1.67% (which were the shortest possible intervals) were insufficient to draw precise conclusions about crystal deformation around the yield region because some changes can occur within a strain range of a few percent. We expect that complementary information could be obtained from position scan measurements at the necking region for ex situ elongated films (see Fig. 6). The elongated dumbbell-shaped samples contain three regions: non-elongated, well-elongated (drawing), and boundary regions (necking). We measured SAXS at the positions marked in Fig. 6. The width of the necking region was greater in β-film than in α-film. Another difference between these films was that the drawing region of the α-film was transparent, whereas that of the β-film appeared white or opaque. The opacity of the β-film is due to microvoids. The longer necking may be related to several events occurring in the β-film depending on stress, some of which occur sequentially. As shown in Figs. 1–3, microvoids start to form first; next, β–α transformation consumes most of the parallel β-lamellae; and finally, the deformation of the perpendicular β-lamellae accompanies β–α transformation. On the other hand, fragmentation and rearrangement of the α-lamellae occur in the α-film.

The middle panels of Fig. 6 show 2D-SAXS images for α- and β-films. There are two major differences between the films. The α-film showed decreased intensity at 0.1 mm, and meridional scattering appeared at 0.2 mm, whereas the β-film did not lose intensity and showed very slow change. At 0.1 mm, some lamellar orientation was observed in the β-film. At this position, the sample was already deformed, as shown in the upper image, and this deformation caused the orientation. At 0.2 mm, nothing happened and the SAXS

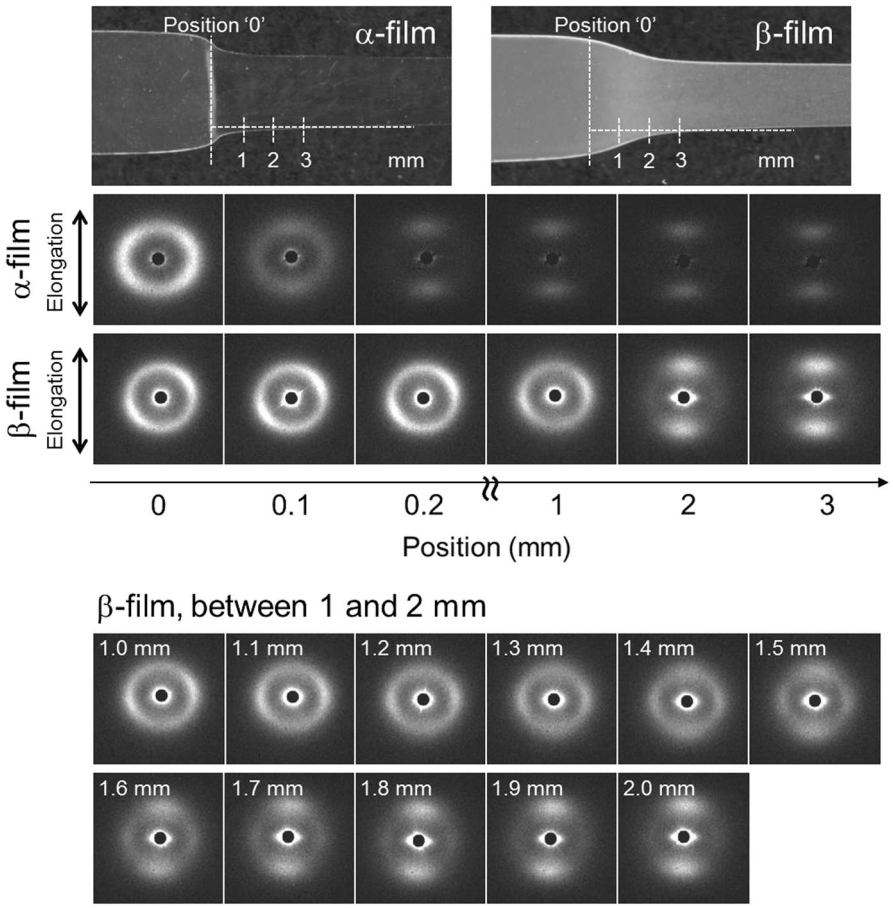


**Fig. 6** Comparison of the dumbbell-shaped films between the α- and β-films and the measured positions, as well as the 2D-SAXS images

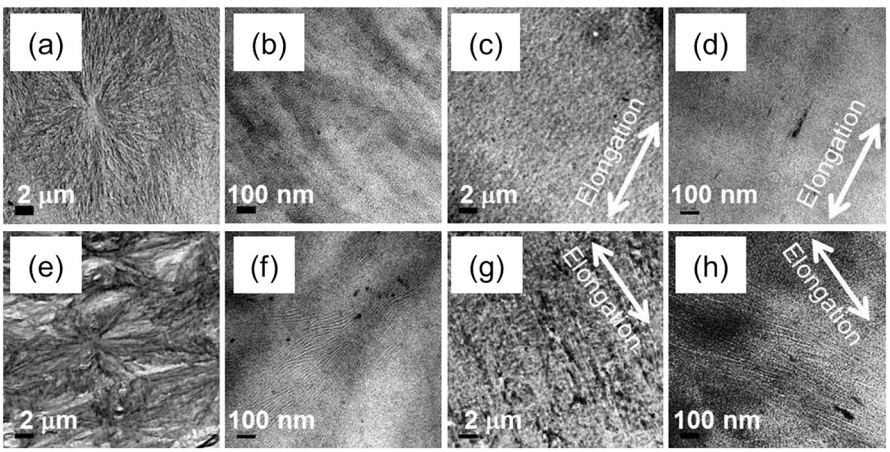


**Fig. 7** Comparison of TEM images between the α- and β-films before and after elongation at 115 °C. **a** and **b** are for α-films before elongation, **e** and **f** are for β-films before elongation, **c** and **d** are for α-films after elongation and **g** and **h** are for β-films after elongation

was almost the same as at 0 mm. The equatorial scattering seemed to appear at 1 mm and then changed to meridional scattering at 2.0 mm. The bottom pictures are 2D-SAXS images for β-film between 1.0 and 2.0 mm. The meridional SAXS seemed to disappear at 1.2 and 1.3 mm, and then, the equatorial SAXS started to disappear between 1.4 and 1.5 mm. This order is consistent with TR-SAXS: the perpendicular β-lamellae remained intact due to microvoid formation, and the parallel β-lamellae were the source of β–α transformation.

## TEM measurement

Figure 7 shows a comparison of the TEM images before and after 200% elongation for the two films. It is clear that spherulites formed before elongation in both films (a and e).

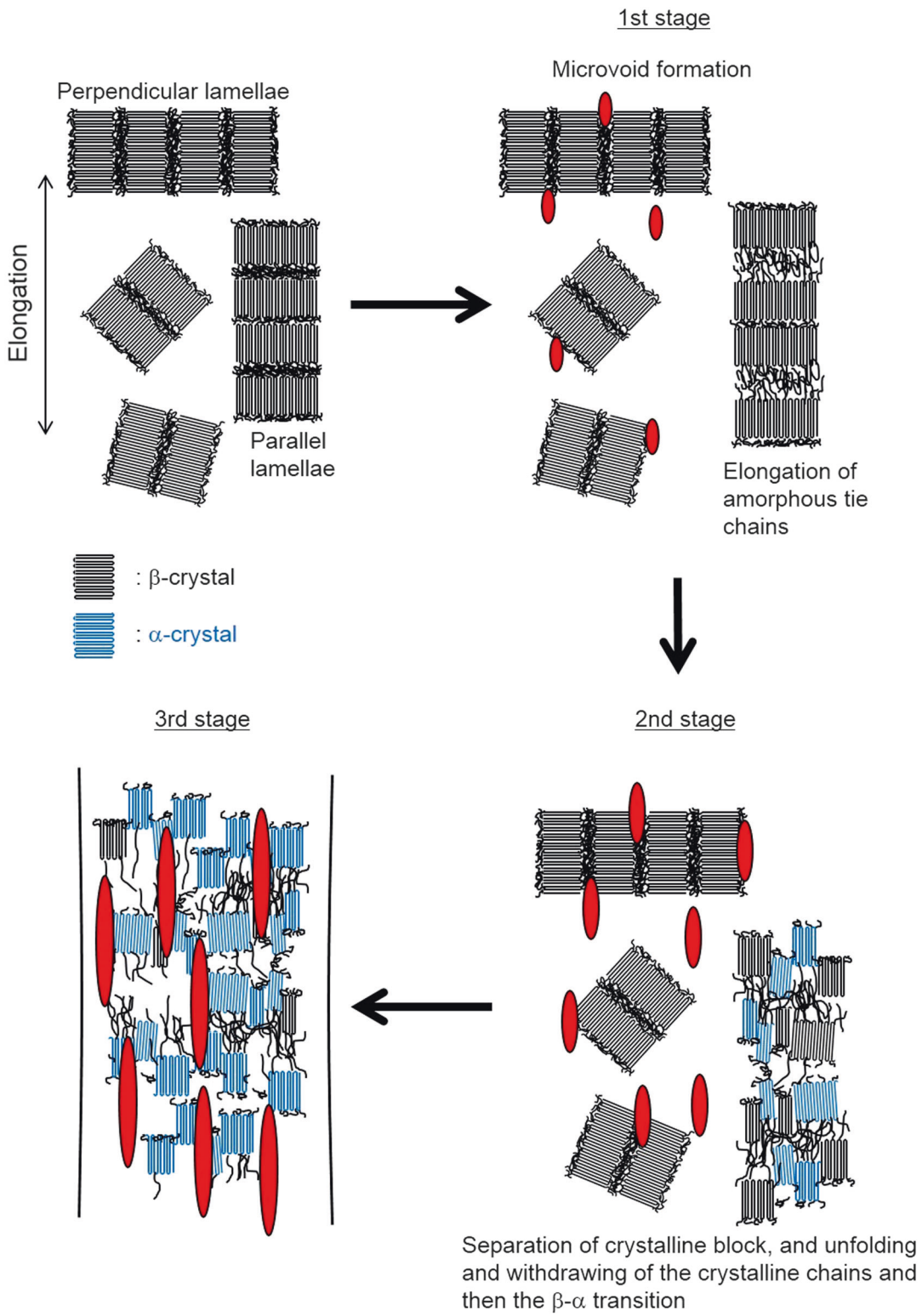


**Fig. 8** Schematic mechanism for elongation induced β- to α-crystalline transformation and microvoid formation

These spherulites were completely destroyed by the elongation (c and g). Clear differences between the α- and β-films are shown in d and h. Specifically, in the β-film, a fibril-like structure in the direction of elongation was observed, whereas there was no such object in the α-film. This indicates that the α-lamellar crystal was fragmented to a very small size (100 nm at most) during the tensile deformation. As discussed above, the α-crystal underwent separation of crystalline block

and interlamellar slipping, which eventually destroyed the lamellar stacking and fragmentation of the crystalline blocks (the so-called lamellar clustering process proposed by Nitta [17]). These small fragmented clusters may not be apparent from TEM.

## Summary

SAXS and WAXS indicated that there were approximately three different stages in the deformation of the β-film, as illustrated in Fig. 8. In the first stage, microvoid formation started at the upper yield point. The applied stress elongates the tie chains in the amorphous domain, especially those in the lamellae parallel to the elongation direction. The lamellae perpendicular to the elongation may be associated with microvoid formation. In the second stage, the meridional β-lamellar SAXS from the lamellae parallel to the elongation decreased, and β–α polymorphous transformation produced a highly oriented α-crystal parallel to the elongation direction. In this stage, the equatorial SAXS from the lamellae perpendicular to the elongation remained almost intact, mainly because of microvoid formation. In the third stage, decreasing equatorial SAXS and re-emerged meridional SAXS were observed. After the disappearance of the parallel lamellae, the remaining perpendicular lamellae served as the source of the transformation. The β-crystal film contained many microvoids, which absorbed the stress. This means the β- and α-crystals may not have been fully subjected to the applied stress, causing lower orientation of the α-crystals and remaining β-crystals.

### Compliance with ethical standards

**Conflict of interest** The authors declare that they have no conflict of interest.

## References


1. Malpass, DB & Band, E. Introduction to industrial polypropylene: properties, catalysts processes. (John Wiley & Sons, New York, 2012).
2. Pasquini, N ed. Polypropylene Handbook. 2nd edn. (Carl Hanser Verlage, Munich, 2005).
3. Androsch R, Di Lorenzo ML, Schick C, Wunderlich B. Mesophases in polyethylene, polypropylene, and poly (1-butene). Polymer. 2010;51:4639–62.
4. Zhang Z, Chen C, Wang C, Junping Z, Mai K. A novel highly efficient β-nucleating agent for polypropylene using nano-CaCO3 as a support. Polym Int. 2010;59:1199–204.
5. Huo H, Jiang S, An L, Feng J. Influence of shear on crystallization behavior of the β phase in isotactic polypropylene with β-nucleating agent. Macromolecules. 2004;37:2478–83.
6. Dragaun H, Hubeny H, Muschik H. Shear-induced β-form crystallization in isotactic polypropylene. J Polym Sci: Polym Phys Ed. 1977;15:1779–89.
7. Turner-Jones A, Aizlewood JM, Beckett D. Crystalline forms of isotactic polypropylene. Die Makromol Chem: Macromol Chem Phys. 1964;75:134–54.
8. Huy TA, Adhikari R, Lüpke T, Henning S, Michler GH. Molecular deformation mechanisms of isotactic polypropylene in α-and β-crystal forms by FTIR spectroscopy. J Polym Sci Part B: Polym Phys. 2004;42:4478–88.
9. Cai Z, et al. Real time synchrotron SAXS and WAXS investigations on temperature related deformation and transitions of β-iPP with uniaxial stretching. Polymer. 2012;53:1593–601.
10. Chu F, Yamaoka T, Kimura Y. Crystal transformation and micropore formation during uniaxial drawing of β-form polypropylene film. Polymer. 1995;36:2523–30.
11. Lin Y, et al. A semi-quantitative deformation model for pore formation in isotactic polypropylene microporous membrane. Polymer. 2015;80:214–27.
12. Varga J. β-modification of isotactic polypropylene: preparation, structure, processing, properties, and application. J Macromol Sci Part B. 2002;41:1121–71.
13. Li J, Cheung W, Chan CM. On deformation mechanisms of β-polypropylene 2. Changes of lamellar structure caused by tensile load. Polymer. 1999;40:2089–102.
14. Li J, Cheung W, Chan CM. On deformation mechanisms of β-polypropylene 3. Lamella structures after necking and cold drawing . Polymer. 1999;40:3641–56.
15. Bohaty P, Vlach B, Seidler S, Koch T, Nezbedova E. Essential work of fracture and the phase transformation in β-iPP. J Macromol Sci, Part B. 2002;41:657–69.
16. Auriemma, F et al. Polymer Crystallization I From Chain Microstructure to Processing. In: Advances in Polymer Science. Springer, Cham, 2016. p. 45–92.
17. Nitta KH, Takayanagi M. Tensile yield of isotactic polypropylene in terms of a lamellar-cluster model. J Polym Sci Part B: Polym Phys. 2000;38:1037–44.
18. Phulkerd P, Hagihara H, Nobukawa S, Uchiyama Y, Yamaguchi M. Plastic deformation behavior of polypropylene sheet with transversal orientation. J Polym Sci Part B: Polym Phys. 2013;51:897–906.
19. Chen Y, et al. Deformation behavior of oriented β-crystals in injection-molded isotactic polypropylene by in situ X-ray scattering. Polymer. 2016;84:254–66.
20. Masunaga H, et al. Multipurpose soft-material SAXS/WAXS/GISAXS beamline at SPring-8. Polym J. 2011;43:471–7.
21. Ogawa H, et al. Experimental station for multiscale surface structural analyses of soft-material films at SPring-8 via a GIS-WAX/GIXD/XR-integrated system. Polym J. 2013;45:109.
22. Nozue Y, Shinohara Y, Ogawa Y, Sakurai T, Hori H, Kasahara T, et al. Deformation behavior of isotactic polypropylene spherulite during hot drawing investigated by simulataneous microbeam SAXS-WAXS and POM measurement. Macromolecules. 2007;40:2036–45.
23. Chu F, Kimura Y. Structure and gas permeability of microporous films prepared by biaxial drawing of β-form polypropylene. Polymer. 1996;37:573–9.